Sinusoidal Signal Estimation from a Noisy-Biased Measurement by an Enhanced PLL with Generalized Error Filtering

Gilberto Pin, Masoud Karimi-Ghartemani, Boli Chen, and Thomas Parisini

***Abstract*— In this paper, an Enhanced Phase-Locked Loop (EPLL) architecture is proposed to deal with the problem of estimating the amplitude, the frequency and the phase of a sinusoidal signal from a noisy measurement. The EPLL scheme is chacterized by an error filter and a phase-feedforward term that are embedded in the estimation algorithm for improved noise rejection and transient performances. By designing the error filter and by selecting the parameters of the PLL according to the guidelines suggested by the stability proof, the technique addressed in the paper allows to cope with the presence of measurement bias while damping the effect of high-frequency noise and harmonics. Simulation comparisons show the effectiveness of the proposed estimation technique.**

I. Introduction

The problem of estimating the Amplitude, the Frequency and the Phase (AFP) of a sinusoidal signal or to reconstruct a pure sinusoid from a noisy measurement is encountered in many engineering fields including power conversion systems (see, for example [1]), measurement and monitoring of electrical systems (see [2]–[4]) and active noise and vibration control (see, for instance [5]). Quite a large variety of AFP approaches are already available in the systems and control community that exploit concepts and tools such as state-variable filtering [6], adaptive observers [7], [8], adaptive notch filters [9] or Extended Kalman filters [10]. On the other hand, in several application contexts of electrical and electronic engineering, the Phase-Locked-Loop (PLL) method and its many variants still remains the preferred choice (see, for instance [11], [12], and the references cited therein). The most important features that render PLL such a widely used architecture are its robustness to environmental and measurement noise, the ease of implementation in digital signal processing platforms and, referring to electrical systems, the applicability to both single and three-phase systems. However, the aforementioned methods based on the PLL architecture can only deal with unbiased signals, while it is commonly acknowledged that both structured perturbation and unstructured noise are encountered in several practical applications (see the very recent paper [13]). In this connection, several recent approaches have been devoted to design robust AFP algorithms able to cope with bias and drift in the measurement (see, for example, [14]–[18]).

Besides the previously-mentioned inability to deal with biased signals, the conventional PLL also exhibits the well-known double-frequency ripple phenomenon, which causes undesired oscillations on the reconstructed signal. A modified PLL architecture conceived to solve this problem is the Magnitude PLL (MPLL) described in [19]; this method consists in providing the PLL of an outer adaptation loop which is in charge of estimating the amplitude of the input signal. Another quite successful approach, which has been conceived with particular focus on power and energy applications, is the Enhanced PLL (EPLL) proposed in [1]. The stability of the EPLL dynamics has been studied in [20]. Extension of the EPLL to address the presence of a DC component (i.e., measurement bias) is presented in [21] by including an additional integrator in the EPLL. Finally, in [22], multiple EPLL units are placed within one "esternal" loop in order to estimate and reject harmonics and inter-harmonics.

In the present work, we introduce an improvement over the original EPLL scheme, consisting of an additional error filter and a phase-feedforward term which is aimed at improving the robustness (phase margin) and the transient performances of the estimator. The proposed architecture is named the *Generalized filtering EPLL* (GEPLL). By properly selecting the structure of the error filter, the biased AFP problem can be addressed as special case. Depending on the transfer function of the error filter, the impact of the phase-feedforward term can be crucial to improve the transient dynamic performance. The stability of the GEPLL is assessed by a two-time scales averaging analysis, that also provides some useful tuning guidelines for the gains of the GEPLL. Simulation results also reporting some comparisons with other techniques show the effectiveness of the proposed approach.

II. The AFP Problem and the GEPLL

Consider a sinusoidal signal $y^*(t)$, generated by the following oscillatory dynamic system:

$$\begin{cases} \dot{\vartheta}^*(t) &= \omega^*, \\ y^*(t) &= A^* \sin(\vartheta^*(t)) \end{cases}, \quad t \in \mathbb{R}_{\geq 0} \tag{1}$$

with $\vartheta^*(0) = \vartheta_0^*$ and where A^*, ω^*, and ϑ_0^* denote the amplitude, the angular frequency, and the initial phase, respectively. While the pure sinusoidal signal y^* is not directly measurable, the following perturbed signal is instead available for performing the AFP estimation:

$$y(t) = y^*(t) + y_0 + \eta(t), \tag{2}$$

where $y_0 \in \mathbb{R}$ denotes the unknown bias, $\eta(t)$ denotes a high-frequency noise, i.e., a signal whose spectral density in the band $(0, \omega^*)$ is negligible. The sum of bias and noise will be denoted by

$$p(t) \triangleq y_0 + \eta(t)$$

and represents the total measurement perturbation signal.

A block diagram of the proposed GEPLL architecture is shown in Fig. 1.The main idea underlying the proposed GEPLL technique consists in embedding in the EPLL structure (see [1]) a linear filter in order to cancel the unknown bias and to dampen the high-frequency perturbations; at the same time, it compensates the phase-shift introduced by the above filter by a phase-feedforward term which enters the

G. Pin is with Electrolux Professional S.p.A., Italy (gilbertopin@alice.it); M. Karimi-Ghartemani is with the Department of Electrical and Computer Engineering, Mississippi State University, USA (karimi@ece.msstate.edu); B. Chen is with Imperial College London, UK (boli.chen10@imperial.ac.uk); T. Parisini is with Imperial College London, UK and also with University of Trieste, Italy (t.parisini@gmail.com).

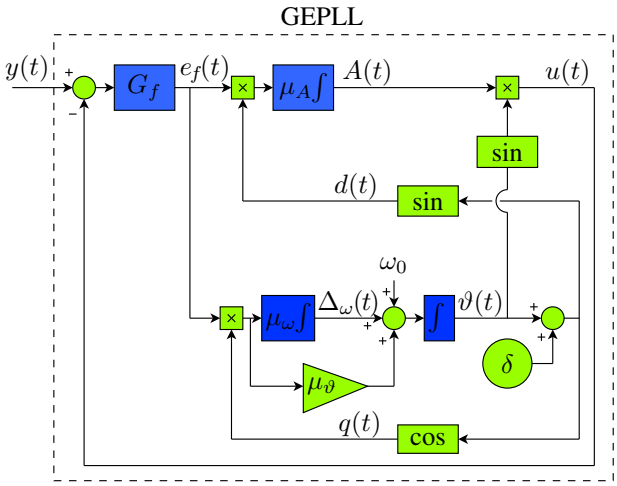

Fig. 1. Detailed scheme of the GEPLL. Compared to the EPLL scheme it contains the customizable error filter $G_f(s)$ and the phase-feedforward δ.

loop through the synchronizing and quadrature signals of the PLL.

In analogy with the EPLL architecture, the GEPLL is fed by the error signal

$$e(t) = y(t) - u(t) = y^* + p(t) - u(t)$$

between the measurement $y(t)$ and the estimated (extracted) sinusoid $u(t) = A(t)\sin(\vartheta(t))$, where $\vartheta(t)$ is the estimated phase angle and $A(t)$ the estimated amplitude. The GEPLL uses a linear time-invariant (LTI) filter to attenuate the effect of the perturbation $p(t)$ on $e(t)$. The filtered error $e_f(t)$ is defined as the output of the following filter:

$$\begin{cases} \dot{x}(t) = \mathbf{A}_f x(t) + \mathbf{b}_f\, e(t), \\ e_f(t) = \mathbf{c}_f^\top x(t) + d_f\, e(t) \end{cases}, \quad t \in \mathbb{R}_{\geq 0} \tag{3}$$

where $x(0) = x_0$. In (3), $x(t) \in \mathbb{R}^n$ is the state vector of the filter; $\mathbf{A}_f$ is an $n \times n$ matrix; $\mathbf{b}_f$ and $\mathbf{c}_f$ are $n \times 1$ vectors; and d_f is a scalar. The order of the filter (3) and the matrices describing its dynamics can be chosen arbitrarily by the designer according to the specifications. By now, we only make the mild assumptions that (3) is reachable, observable and that $\mathbf{A}_f$ is Hurwitz. In the Laplace domain, the filter (3) can be described by the stable transfer function:

$$G_f(s) = \mathbf{c}_f^\top (s\mathbf{I} - \mathbf{A}_f)^{-1}\mathbf{b}_f + d_f. \tag{4}$$

The amplitude, frequency and phase-angle dynamics of the GEPLL are described by

$$\begin{cases} \dot{A}(t) = \mu_A\, d(t)\, e_f(t) \\ \dot{\Delta}_\omega(t) = \mu_\omega\, q(t)\, e_f(t) \\ \dot{\vartheta}(t) = \omega_0 + \Delta_\omega(t) + \mu_\vartheta\, q(t)\, e_f(t) \end{cases}, \quad t \in \mathbb{R}_{\geq 0}\,, \tag{5}$$

with $A(0) = A_0$, $\vartheta(0) = \vartheta_0$, $\Delta_\omega(0) = 0$ and where $\Delta_\omega(t)$ represents the frequency correction generated by the algorithm with respect to the nominal frequency ω_0, such that the estimated frequency is given by $\omega(t) = \Delta_\omega(t) + \omega_0$. The terms

$$d(t) = \sin(\vartheta(t) + \delta)\,; \quad q(t) = \cos(\vartheta(t) + \delta)\,; \tag{6}$$

are called respectively the *direct* and the *quadrature* synchronizing signals, while $\delta = \angle G_f(i\omega_0)$ is the phase of the filter at the nominal frequency. The constants μ_A, μ_ϑ, $\mu_\omega \in \mathbb{R}_{>0}$ in (5) are tuning gains to be set according to the stability analysis that will be carried out in the sequel.

The phase-feedforward parameter $\delta \in \mathbb{R}$ in (6) (not present in EPLL scheme) accounts for the phase shift introduced by the filter (3) at the nominal frequency ω_0. This term can have significant impact on the transient response and on the stability properties of the estimator.

III. Averaging Stability Analysis of the GEPLL

The following constraints are introduced to simplify the stability analysis of the GEPLL:

1) Admissible frequency interval:

$$\omega(t) \in [\omega_{\min}, \omega_{\max}], \text{with } 0 < \omega_{\min} \leq \omega_{\max},$$

which can be accomplished simply by clipping the frequency correction variable $\Delta_\omega(t)$ within the interval $[\omega_{\min} - \omega_0, \omega_{\max} - \omega_0]$, where $\omega_{\min}$, and $\omega_{\max}$ are a-priori known bounds on the true frequency of the sinusoid;

2) Amplitude positivity: $A(t) \geq 0$.

Let $g_f(t)$ denote the impulse response of $G_f(s)$. Then:

$$e_f(t) = g_f(t) \circledast e(t) \tag{7}$$

where $\circledast$ denotes the standard convolution operator in the time-domain. Introducing the phase reconstruction error $\tilde{\vartheta}(t) \triangleq \vartheta(t) - \vartheta^*(t)$, the amplitude error $\tilde{A}(t) \triangleq A(t) - A^*$ and the frequency estimation error $\tilde{\omega}(t) \triangleq \omega(t) - \omega^* = \omega_0 + \Delta_\omega(t) - \omega^*$, the tracking error $e(t)$ is given by

$$\begin{aligned} e(t) \;=\; & -\tilde{A}(t)\sin\big(\vartheta(t)\big) - A^*\cos\big(\vartheta(t)\big)\sin\big(\tilde{\vartheta}(t)\big) \\ & + A^*\sin\big(\vartheta(t)\big)\Big[\cos\big(\tilde{\vartheta}(t)\big) - 1\Big] + p(t). \end{aligned} \tag{8}$$

By substituting (8) in (7) and (5) and by expanding the synchronizing signals (6), the error dynamics becomes

$$\begin{aligned} \dot{\tilde{A}}(t) = \mu_A \Big\{ & \sin\Big(\vartheta^*(t) + \tilde{\vartheta}(t)\Big)\cos(\delta) + \cos\Big(\vartheta^*(t) + \tilde{\vartheta}(t)\Big)\sin(\delta) \Big\} \times \\ \Big(g_f(t) \circledast \Big\{ & -\tilde{A}(t)\sin\Big(\vartheta^*(t) + \tilde{\vartheta}(t)\Big) - A^*\cos\Big(\vartheta^*(t) + \tilde{\vartheta}(t)\Big)\sin\Big(\tilde{\vartheta}(t)\Big) \\ & + A^*\sin\Big(\vartheta^*(t) + \tilde{\vartheta}(t)\Big)\Big[\cos\Big(\tilde{\vartheta}(t)\Big) - 1\Big] + p(t) \Big\} \Big), \end{aligned} \tag{9}$$

$$\begin{aligned} \dot{\tilde{\omega}}(t) = \mu_\omega \Big\{ & \cos\Big(\vartheta^*(t) + \tilde{\vartheta}(t)\Big)\cos(\delta) - \sin\Big(\vartheta^*(t) + \tilde{\vartheta}(t)\Big)\sin(\delta) \Big\} \times \\ \Big(g_f(t) \circledast \Big\{ & -\tilde{A}(t)\sin\Big(\vartheta^*(t) + \tilde{\vartheta}(t)\Big) - A^*\cos\Big(\vartheta^*(t) + \tilde{\vartheta}(t)\Big)\sin\Big(\tilde{\vartheta}(t)\Big) \\ & + A^*\sin\Big(\vartheta^*(t) + \tilde{\vartheta}(t)\Big)\Big[\cos\Big(\tilde{\vartheta}(t)\Big) - 1\Big] + p(t) \Big\} \Big), \end{aligned} \tag{10}$$

$$\dot{\tilde{\vartheta}}(t) = \frac{\mu_\vartheta}{\mu_\omega}\,\dot{\tilde{\omega}}(t) + \tilde{\omega}(t)\,, \tag{11}$$

where (11) has been recast in terms of the derivatives of the other state variables for the sake of brevity. Now, let us introduce an additional auxiliary state variable $v'(t)$ obtained by filtering the frequency error $\dot{v}'(t) = -\mu_v v'(t) + \tilde{\omega}(t)$, where $\mu_v > 0$ is a constant parameter. Then, defining $\tilde{\psi}(t) \triangleq \tilde{\vartheta}(t) - v'(t)$, the time-derivative of $\tilde{\vartheta}(t)$ results in

$$\dot{\tilde{\psi}}(t) = \frac{\mu_\vartheta}{\mu_\omega}\dot{\tilde{\omega}}(t) + \mu_v\, v'(t)\,.$$

Substituting $\tilde{\vartheta} \to \tilde{\psi} + v'$ in (9)-(11), letting $\mu_A = \epsilon\lambda_A$, $\mu_\omega = \epsilon\lambda_\omega$, $\mu_\vartheta = \epsilon\lambda_\vartheta$, $\lambda_v = \mu_v/\epsilon$ for some $\epsilon \in \mathbb{R}_{>0}$, and dropping, again for the sake of the brevity, the dependence

of the error variables and $v^{'}$ on time, we obtain the following autonomous nonlinear dynamical system:

$$\begin{array}{rl} \dot{\tilde{A}} = & \epsilon f^{'}{}_A(t,\tilde{A},\tilde{\omega},\tilde{\psi},v^{'}) \\ \dot{\tilde{\omega}} = & \epsilon f^{'}{}_\omega(t,\tilde{A},\tilde{\omega},\tilde{\psi},v^{'}) \\ \dot{\tilde{\psi}} = & \epsilon f^{'}{}_\psi(t,\tilde{A},\tilde{\omega},\tilde{\psi},v^{'}) \\ \dot{v}^{'} = & -\mu_v\, v^{'} + \tilde{\omega} \end{array} \tag{12}$$

where

$$\begin{aligned} f^{'}{}_A(t,\tilde{A},\tilde{\omega},\tilde{\psi},v^{'}) \triangleq\, & \lambda_A \Big\{ \sin(\vartheta^*)\kappa_1 + \cos(\vartheta^*)\kappa_2 \Big\} \\ & \times g_f(t) \circledast \Big\{ p(t) + \sin(\vartheta^*)\kappa_3 + \cos(\vartheta^*)\kappa_4 \Big\}, \end{aligned}$$

$$\begin{aligned} f^{'}{}_\omega\left(t,\tilde{A},\tilde{\omega},\tilde{\psi},v^{'}\right) \triangleq\, & \lambda_\omega \Big\{ \cos(\vartheta^*)\kappa_1 - \sin(\vartheta^*)\kappa_2 \Big\} \\ & \times g_f(t) \circledast \Big\{ p(t) + \sin(\vartheta^*)\kappa_3 + \cos(\vartheta^*)\kappa_4 \Big\}, \end{aligned}$$

$$f^{'}{}_\psi\left(t,\tilde{A},\tilde{\omega},\tilde{\psi},v^{'}\right) \triangleq \frac{\lambda_\vartheta}{\lambda_\omega}\frac{\dot{\tilde{\omega}}}{\epsilon} + \lambda_v\, v^{'}$$

with

$$\begin{aligned} \kappa_1 \;\triangleq\;& \cos\big(\tilde{\psi}+v^{'}\big)\cos(\delta) - \sin\big(\tilde{\psi}+v^{'}\big)\sin(\delta), \\ \kappa_2 \;\triangleq\;& \cos\big(\tilde{\psi}+v^{'}\big)\sin(\delta) + \sin\big(\tilde{\psi}+v^{'}\big)\cos(\delta), \\ \kappa_3 \;\triangleq\;& -\tilde{A}\cos\big(\tilde{\psi}+v^{'}\big) + A^*\sin\big(\tilde{\psi}+v^{'}\big)\sin\big(\tilde{\psi}+v^{'}\big) \\ & + A^*\cos\big(\tilde{\psi}+v^{'}\big)\cos\big(\tilde{\psi}+v^{'}\big) - A^*\cos\big(\tilde{\psi}+v^{'}\big), \\ \kappa_4 \;\triangleq\;& -\tilde{A}\sin\big(\tilde{\psi}+v^{'}\big) - A^*\cos\big(\tilde{\psi}+v^{'}\big)\sin\big(\tilde{\psi}+v^{'}\big) \\ & + A^*\sin\big(\tilde{\psi}+v^{'}\big)\cos\big(\tilde{\psi}+v^{'}\big) - A^*\sin\big(\tilde{\psi}+v^{'}\big)\,. \end{aligned}$$

System (12) can be recast into a *mixed-time scale* form (see [23]) by introducing the *slow-state* $\mathbf{x} \triangleq [\tilde{A},\tilde{\omega},\tilde{\psi}]^\top$. Thus:

$$\left\{ \begin{array}{rcl} \dot{\mathbf{x}} &=& \epsilon\, \mathbf{f}^{'}(t,\mathbf{x},v^{'}) \\ \dot{v}^{'} &=& -\mu_v v^{'} + h\,(\mathbf{x}) \end{array} \right. \tag{13}$$

where $v^{'}$ is the *fast-state*, $h : \mathbb{R}^3 \to \mathbb{R}$ is a linear function $h(\mathbf{x}) = [0\ 1\ 0]\mathbf{x} = \tilde{\omega}$ and $\mathbf{f}^{'} : \mathbb{R}\times\mathbb{R}^3\times\mathbb{R} \to \mathbb{R}^3$ is given by

$$\mathbf{f}^{'}(t,\mathbf{x},v^{'}) \triangleq \left[\begin{array}{c} f^{'}{}_A(t,\tilde{A},\tilde{\omega},\tilde{\psi},v^{'}) \\ f^{'}{}_\omega(t,\tilde{A},\tilde{\omega},\tilde{\psi},v^{'}) \\ f^{'}{}_\psi(t,\tilde{A},\tilde{\omega},\tilde{\psi},v^{'}) \end{array} \right].$$

We proceed by determining the averaged system associated to (13). First, we compute the integral functions $v(t,\overline{\mathbf{x}}) : \mathbb{R}\times\mathbb{R}^3 \to \mathbb{R}$ and $\mathbf{f}(t,\overline{\mathbf{x}}) : \mathbb{R}\times\mathbb{R}^3 \to \mathbb{R}^3$ as follows:

$$v(t,\overline{\mathbf{x}}) \triangleq \int_0^t e^{-\mu_v(t-\tau)} h\,(\overline{\mathbf{x}})\, d\tau, \tag{14}$$

with $\overline{\mathbf{x}} \in \mathbb{R}^3$ taken as a constant in the integration and $\mathbf{f}(t,\overline{\mathbf{x}}) = \mathbf{f}^{'}(\tau,\overline{\mathbf{x}},v(\tau,\overline{\mathbf{x}}))$. The averaged-slow transition function is given by

$$\mathbf{f}_{av}(\overline{\mathbf{x}}) \triangleq \lim_{T\to\infty}\frac{1}{T}\int_0^T \mathbf{f}(\tau,\overline{\mathbf{x}})\, d\tau.$$

The averages for the following scalar function components

$$\mathbf{f}\,(t,\overline{\mathbf{x}}) = \left[\begin{array}{c} f_A\ (t,\overline{A},\overline{\omega},\overline{\psi}) \\ f_\omega\ (t,\overline{A},\overline{\omega},\overline{\psi}) \\ f_\psi\ (t,\overline{A},\overline{\omega},\overline{\psi}) \end{array} \right],$$

can be computed based on the fact that (14) yields

$$v(t,\overline{\mathbf{x}}) = {\mu_v}^{-1}\,\overline{\omega}\,(1 - e^{-\mu_v t}) \tag{15}$$

Moreover, if the filter is properly selected to cancel asymptotically the bias and to attenuate the high-frequency noise by low-pass filtering, then we can use the following approximation[1] to simplify the analysis

$$\lim_{T\to\infty}\frac{1}{T}\int_0^T w(t)\big(g_f(t)\circledast p(t)\big)\, dt \approx 0, \tag{16}$$

where $w(t)$ is any integrable function such that $\lim_{T\to\infty}\frac{1}{T}\int_0^T |w(t)|dt < \infty$. The overall averaged vector function can be written as

$$\mathbf{f}_{av}(\overline{x}) = \left[\begin{array}{c} f_{A\,av}(\overline{A},\overline{\omega},\overline{\psi}) \\ f_{\omega\,av}(\overline{A},\overline{\omega},\overline{\psi}) \\ f_{\psi\,av}(\overline{A},\overline{\omega},\overline{\psi}) \end{array} \right]. \tag{17}$$

with the single components given by

$$f_{A_{av}}\left(\overline{A},\overline{\omega},\overline{\psi}\right) = \frac{\lambda_A}{2}\left[G_{f_R^*}(\bar{\kappa}_1\bar{\kappa}_3 + \bar{\kappa}_2\bar{\kappa}_4) + G_{f_I^*}(\bar{\kappa}_2\bar{\kappa}_3 - \bar{\kappa}_1\bar{\kappa}_4) \right] \tag{18}$$

$$f_{\omega_{av}}\left(\overline{A},\overline{\omega},\overline{\psi}\right) = \frac{\lambda_\omega}{2}\left[G_{f_R^*}(\bar{\kappa}_1\bar{\kappa}_4 - \bar{\kappa}_2\bar{\kappa}_3) + G_{f_I^*}(\bar{\kappa}_1\bar{\kappa}_3 + \bar{\kappa}_2\bar{\kappa}_4) \right] \tag{19}$$

$$f_{\psi_{av}}\left(\overline{A},\overline{\omega},\overline{\psi}\right) = \frac{\lambda_\vartheta}{\lambda_\omega} f_{\omega_{av}}\left(\overline{A},\overline{\omega},\overline{\psi}\right) + \frac{\overline{\omega}}{\epsilon}. \tag{20}$$

in which we have used the notation $G_{f_R^*} = \mathrm{Re}\,(G_f(i\,\omega^*))$, $G_{f_I^*} = \mathrm{Im}\,(G_f(i\,\omega^*))$, and we defined

$$\begin{aligned} \bar{\kappa}_1 \;\triangleq\;& \cos\Big(\overline{\psi}+\frac{\overline{\omega}}{\mu_v}\Big)\cos(\delta) - \sin\Big(\overline{\psi}+\frac{\overline{\omega}}{\mu_v}\Big)\sin(\delta) \\ \bar{\kappa}_2 \;\triangleq\;& \cos\Big(\overline{\psi}+\frac{\overline{\omega}}{\mu_v}\Big)\sin(\delta) + \sin\Big(\overline{\psi}+\frac{\overline{\omega}}{\mu_v}\Big)\cos(\delta) \\ \bar{\kappa}_3 \;\triangleq\;& -\overline{A}\cos\Big(\overline{\psi}+\frac{\overline{\omega}}{\mu_v}\Big) + A^*\sin\Big(\overline{\psi}+\frac{\overline{\omega}}{\mu_v}\Big)\sin\Big(\overline{\psi}+\frac{\overline{\omega}}{\mu_v}\Big) \\ & + A^*\cos\Big(\overline{\psi}+\frac{\overline{\omega}}{\mu_v}\Big)\cos\Big(\overline{\psi}+\frac{\overline{\omega}}{\mu_v}\Big) - A^*\cos\Big(\overline{\psi}+\frac{\overline{\omega}}{\mu_v}\Big) \\ \bar{\kappa}_4 \;\triangleq\;& -\overline{A}\sin\Big(\overline{\psi}+\frac{\overline{\omega}}{\mu_v}\Big) - A^*\cos\Big(\overline{\psi}+\frac{\overline{\omega}}{\mu_v}\Big)\sin\Big(\overline{\psi}+\frac{\overline{\omega}}{\mu_v}\Big) \\ & + A^*\sin\Big(\overline{\psi}+\frac{\overline{\omega}}{\mu_v}\Big)\cos\Big(\overline{\psi}+\frac{\overline{\omega}}{\mu_v}\Big) - A^*\sin\Big(\overline{\psi}+\frac{\overline{\omega}}{\mu_v}\Big) \end{aligned}$$

Resorting to the Mixed Time-Scales Averaging Theorem (see [23, Chapter 4]), the stability of an equilibrium point of the error system (13) can be inferred from that of the autonomous-averaged slow system

$$\dot{\overline{\mathbf{x}}} = \epsilon\, \mathbf{f}_{av}(\overline{\mathbf{x}}). \tag{21}$$

Theorem 3.1 (Averaging Stability Theorem): If the averaged system (21) is locally exponentially stable in $\mathbf{x} = \mathbf{0}$, then the error system is in turn locally exponentially stable in the zero-error equilibrium point $(\tilde{A},\tilde{\omega},\tilde{\theta}) = (0,0,0)$, for ϵ sufficiently small. □

Proof: The present stability result follows from the direct application of the Mixed-Time-Scales Averaging Theorem reported in [23, Chapter 4] to the error system. Indeed one can observe that Points i)-v) correspond to Assumptions

[1]The average (16) is exact in presence of DC-bias if the filter $G_f(s)$ has a zero at $s = 0$, in absence of high-frequency noise. Conversely, in presence of high-frequency noise or when the signal is corrupted by higher-order harmonics besides the fundamental, the approximation neglects some residual contribution, whose magnitude depends on the attenuation of the filter at the frequency of the disturbance.

B1-B5 in Section 4.4.1 while Property $vi)$ corresponds to Assumption B6 in Section 4.4.2 of [23]. In this case, however, only local stability at the zero equilibrium point can be inferred from the stability of the averaged system. ■

Now, we need to determine the values of the adaptation gains $\mu_A, \mu_\omega, \mu_\vartheta$ for which the averaged system is locally exponentially stable. The linearized-averaged system around the equilibrium $\overline{\mathbf{x}} = \mathbf{0}$ gives

$$\dot{\overline{\mathbf{x}}} = \mathbf{M}_{A,\omega,\psi}\,\overline{\mathbf{x}}, \tag{22}$$

where $\mathbf{M}_{A,\omega,\psi}$ is the Jacobian of $\mathbf{f}_{av}$ at the equilibrium. This matrix is calculated as

$$\mathbf{M}_{A,\omega,\psi} = \begin{bmatrix} -\mu_A M_1 & \dfrac{\lambda_A}{\lambda_v} M_2 A^* & \mu_A M_2 A^* \\ -\mu_\omega M_2 & -\dfrac{\lambda_\omega}{\lambda_v} M_1 A^* & -\mu_\omega M_1 A^* \\ -\mu_\vartheta M_2 & 1 - \dfrac{\lambda_\vartheta}{\lambda_v} M_1 A^* & -\mu_\vartheta M_1 A^* \end{bmatrix} \tag{23}$$

where $M_1 \triangleq \left[G_{f_R^*}\cos(\delta) + G_{f_I^*}\sin(\delta)\right]/2$ and $M_2 \triangleq \left[G_{f_I^*}\cos(\delta) - G_{f_R^*}\sin(\delta)\right]/2$. Let ω_0 be an "a priori" estimate of ω^*, such that $\omega_0 \in [\omega_{\min}, \omega_{\max}]$. We show that the choice of the phase-feedforward term

$$\delta = \angle G_f(i\,\omega_0) \tag{24}$$

ensures the local stability of the averaged system. Defining the phase compensation error as $\tilde{\delta} \triangleq \delta - \angle G_f(i\,\omega^*)$, we obtain

$$\begin{aligned} G_{f_R^*}\cos(\delta) + G_{f_I^*}\sin(\delta) &= |G(i\,\omega^*)|\cos(\tilde{\delta}), \\ G_{f_I^*}\cos(\delta) - G_{f_R^*}\sin(\delta) &= -|G(i\,\omega^*)|\sin(\tilde{\delta}). \end{aligned} \tag{25}$$

In view of (25) and recalling that $\mu_v = \epsilon\lambda_v$ does not impact the GEPLL equations, by letting $\lambda_v >> \max\{\lambda_A, \lambda_\omega, \lambda_\vartheta\}$, (23) takes on the simpler form:

$$\mathbf{M}_{A,\omega,\psi} = \frac{1}{2}\begin{bmatrix} -\mu_A|G_f(i\,\omega^*)|\cos(\tilde{\delta}) & 0 & -\mu_A|G_f(i\,\omega^*)|A^*\sin(\tilde{\delta}) \\ \mu_\omega|G_f(i\,\omega^*)|\sin(\tilde{\delta}) & 0 & -\mu_\omega|G_f(i\,\omega^*)|A^*\cos(\tilde{\delta}) \\ \mu_\vartheta|G_f(i\,\omega^*)|\sin(\tilde{\delta}) & 1 & -\mu_\vartheta|G_f(i\,\omega^*)|A^*\cos(\tilde{\delta}) \end{bmatrix}, \tag{26}$$

that, remarkably, depends on the phase compensation error $\tilde{\delta}$. In nominal conditions (that is, for a known frequency $\omega_0 \equiv \omega^*$) in view of (24) the phase compensation error is null $(\omega_0 = \omega^*) \Rightarrow (\tilde{\delta} = 0)$. In this scenario, the dynamic behavior of the amplitude error is decoupled from that of the frequency and phase errors, as a result of the substitution $\tilde{\delta} = 0$ in (26), the eigenvalues of $\mathbf{M}_{A,\omega,\vartheta}|_{\tilde{\delta}=0}$ have negative real part if $\mu_A, \mu_\vartheta, \mu_\omega > 0$, which is therefore a sufficient condition for local asymptotic exponential stability in the nominal case. In the more general situation of unknown frequency, it is of primary importance to characterize the robustness of the scheme in presence of a non-null phase compensation error ($\tilde{\delta} \neq 0$) and obtain the range of admissible adaptation gains guaranteeing local stability. Such analysis can be carried out by checking the signs of the Routh array induced by the characteristic polynomial of the linearized averaged system. The characteristic polynomial $r(s)$ of the matrix $\mathbf{M}_{A,\omega,\psi}$ in (26) is given by

$$\begin{aligned} r(s) = s^3 &+ \frac{|G_f(i\,\omega^*)|\cos(\tilde{\delta})}{2}(\mu_A + A^*\mu_\vartheta)\,s^2 \\ &+ \frac{A^*|G_f(i\,\omega^*)|}{4}\Big(\mu_\omega\cos(\tilde{\delta}) + \mu_A\mu_\vartheta|G_f(i\,\omega^*)|\Big)s \\ &+ \frac{A^*\,|G_f(i\,\omega^*)|^2}{8}\mu_A\mu_\omega \ . \end{aligned}$$

Assume that the phase error is bounded in a closed interval[2]

$$\tilde{\delta} \in [-\overline{\delta}, \overline{\delta}], \text{ with } \overline{\delta} \geq 0.$$

According to the Routh-Hurwitz criterion, $r(s)$ is Hurwitz iff the following inequality is verified

$$\begin{aligned} \cos(\tilde{\delta})\Big[|G_f(i\,\omega^*)|\,\mu_A\mu_\vartheta\,(\mu_A + A^*\mu_\vartheta) + A^*\mu_\omega\mu_\vartheta\cos(\tilde{\delta})\Big] \\ -\mu_\omega\mu_A\left(1 - \Big(\cos(\tilde{\delta})\Big)^2\right) > 0, \end{aligned}$$

and considering that

$$\begin{aligned} \cos(\tilde{\delta})\Big[|G_f(i\,\omega^*)|\,\mu_A\mu_\vartheta\,(\mu_A + A^*\mu_\vartheta) + A^*\mu_\omega\mu_\vartheta\cos(\tilde{\delta})\Big] \\ > \ \cos(\tilde{\delta})\,|G_f(i\,\omega^*)|\,{\mu_A}^2\mu_\vartheta, \qquad \forall A^* \geq 0, \end{aligned}$$

then we immediately determine a sufficient condition to render $\mathbf{M}_{A,\omega,\psi}$ a Hurwitz matrix:

$$\cos(\tilde{\delta})\,|G_f(i\,\omega^*)|\,\mu_A\mu_\vartheta - \mu_\omega\left(1 - \Big(\cos(\tilde{\delta})\Big)^2\right) > 0.$$

Hence, it is possible to enforce $\mathbf{M}_{A,\omega,\psi} < 0$ for any possible $A^* > 0$ by picking the frequency adaptation parameter such that

$$0 < \mu_\omega < \frac{|G_f(i\,\omega^*)|\,\mu_\vartheta\mu_A\cos(\tilde{\delta})}{1 - \Big(\cos(\tilde{\delta})\Big)^2}, \ \forall\tilde{\delta} : |\tilde{\delta}| \leq \overline{\delta}. \tag{27}$$

The upper limit in (27) becomes positive unbounded for $\overline{\delta} \to 0$; that is, when the phase compensation error is null, the GEPLL remains stable even with a very large frequency adaptation gain μ_ω. However, the condition $\overline{\delta} \to 0$ is unlikely to be verified in practice, due to the uncertainty in the frequency of the measured signal. When an upper bound $\overline{\delta} : 0 \leq \delta < \pi/2$ on the norm of the phase-compensation error can be established:

$$|\tilde{\delta}| \leq \overline{\delta} < \frac{\pi}{2}, \tag{28}$$

then the constraint (27) reduces to

$$0 < \mu_\omega < \frac{|G_f(i\,\omega^*)|\,\mu_\vartheta\mu_A\cos(\overline{\delta})}{1 - \big(\cos(\overline{\delta})\big)^2}, \tag{29}$$

for which a solution always exists, assuming that the chosen filter $G_f(s)$ does not have zeroes in the admissible frequency range.

The following final remarks are now in place.

Remark 3.1 (Phase compensation bound): Choosing the phase-feedforward δ according to (24), we can rewrite the phase compensation error as

$$\tilde{\delta} = \angle G_f(i\,\omega_0) - \angle G_f(i\,\omega^*). \tag{30}$$

[2]If the filter $G_f(s)$ is chosen as minimum-phase one and the admissible frequency range is bounded in a compact set, then a conservative bound $\overline{\delta}$ can be computed by (31).

Given an admissible frequency range $[\omega_{\min}, \omega_{\max}]$, we can determine the worst-case phase compensation error:

$$\overline{\delta} = \max_{\omega\in[\omega_{\min},\omega_{\max}]} \angle G_f(i\,\omega) - \min_{\omega\in[\omega_{\min},\omega_{\max}]} \angle G_f(i\,\omega), \quad (31)$$

that depends on the specific filter $G_f(s)$ chosen by the designer and on the width of the admissible frequency interval $[\omega_{\min}, \omega_{\max}]$. When the uncertainty on the frequency is large ($\omega_{\min} << \omega_{\max}$), then the last inequality in (28) may not be fulfilled by high-order error filters, and it can be necessary to decrease the filter order to fulfill this condition. Indeed, a first order filter allows to satisfy (28) for an arbitrarily large range of admissible frequencies. For instance, the simplest form of a realizable bias-cancelling filter is

$$G_f s = \frac{s}{s+\mu_0} \quad (32)$$

with $\mu_0 \in \mathbb{R}_{>0}$ arbitrary. The phase-shift introduced by this simple filter at the frequency of the input sinusoid is $\angle G_f(i\omega^*) \in (0, \pi/2)$, for any finite frequency $\omega^* > 0$. It follows that by any choice of the phase-feedforward parameter δ in the interval $(0, \pi/2)$, the phase compensation error verifies $|\tilde{\delta}| < \pi/2$, regardless of the extension of the admissible frequency range. A further filter that can be exploited in case of a large frequency uncertainty is:

$$G_f(s) = \frac{s}{s+\mu_0}\frac{\omega_c}{s+\omega_c}, \quad (33)$$

that increases the ability of the GEPLL to attenuate high frequency harmonics and noise. Here, $\omega_c \in \mathbb{R}_{>0}$ is the cut-off frequency of the additional low-pass filter. The phase-shift introduced by this second-order filter is $\angle G_f(i\omega^*) \in (-\pi/2, \pi/2)$ for any finite frequency $\omega^* > 0$. By choosing a null phase-feedforward parameter ($\delta = 0$) then the worst-case phase compensation error verifies $|\tilde{\delta}| < \pi/2$, regardless of the extension of the admissible frequency range.

Remark 3.2 (Design Guidelines): The first design step consists in choosing the error filter $G_f(s)$ depending on the characteristics of the measurement perturbation, for example to cancel the bias or to attenuate high-frequency noise and harmonics. Relying on some "a priori" informations on the signal such as the nominal frequency ω_0 and a first guess estimate of its amplitude, the designer may choose the parameters μ_A, μ_ω and μ_ϑ in order to assign the nominal poles of the linearized error dynamics (by imposing the eigenvalues of the matrix $\mathbf{M}_{A,\omega,\psi}$). Then, given some reasonable bounds on the frequency of the signal $(\omega_{\min}, \omega_{\max})$ one should check, by inspection, if condition (28) is verified, with $\overline{\delta}$ computed as in (31). If this condition is not verified, one can iterate the above steps by re-designing the filter. As described in Remark 3.1, reducing the order of the filter improves the robustness of the estimator; moreover, condition (28) can be always verified by a first order filter or by a second order filter having the form of (33) with a suitable phase-feedforward. Finally, the gain μ_ω has to be tuned, compared to the nominal design value, in order to fulfill inequality (29). In other terms, in presence of large uncertainty on the frequency of the input sinusoid, the stability of the GEPLL is obtained at the price of decreasing the convergence rate of the frequency estimation dynamics.

IV. Comparative Numerical Examples

Example 1. (*Error filter design and phase-feedforward for bias removal and attenuation of higher-order harmonics*) In this example, three different filter and phase-feedforward designs are considered for comparison: GEPLL1 uses the simple bias-cancelling filter (32) with $G_f(s) = \frac{s}{s+100}$; GEPLL2 uses the two-poles filter (33) with $G_f(s) = \frac{s}{s+100}\frac{300}{s+300}$ with no phase-feedforward, while GEPLL3 uses the same filter of GEPLL2 with $\delta = -0.64$ rad. The PLL gains are $\mu_A = \mu_\vartheta = 300$ and $\mu_\omega = 15 \cdot 10^3$. Figure 2 shows the numerical results including the phase angle estimation errors obtained by the above three GEPLLs. The input signal is a noisy sinusoid affected by two high-frequency harmonics: 10% of harmonic 5 and 10% of harmonic 7. In particular, the fundamental component starts from a pure sine wave with unitary amplitude and 60 Hz frequency. At time $t = 0.1$ s the following changes apply to the input signal: the amplitude jumps to 1.2, the phase jumps from 0 to 90 deg, the frequency increases to 60.4 Hz. Clearly, GEPLL2 and GEPLL3 provide much smoother estimate of the phase angle in the steady state because they involve an attenuation of the harmonics; moreover, GEPLL3 exhibits a much faster transient response than GEPLL2 thanks to the phase-feedforward. The same observation also applies to the frequency and amplitude estimates.

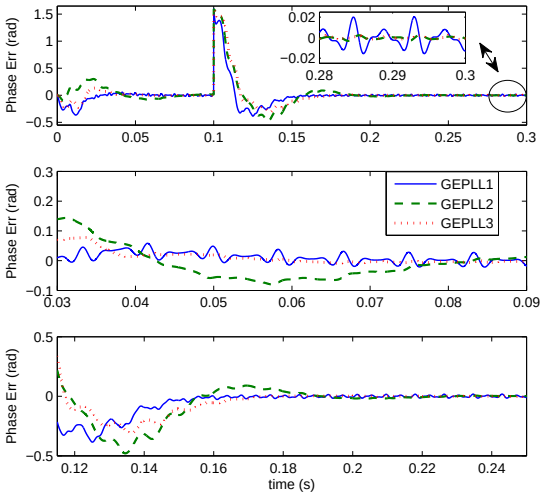

Fig. 2. The top diagram shows the phase angle estimation errors obtained by three GEPLL structures with a perturbed input signal exhibiting a step-wise change in fequency, amplitude and bias at time $t = 0.1s$ (Example 1): GEPLL1 ($G_f = \frac{s}{s+100}$), GEPLL2 ($G_f(s) = \frac{s}{s+100}\frac{300}{s+300}$ and $\delta = 0$), GEPLL3 ($G_f(s) = \frac{s}{s+100}\frac{300}{s+300}$ and $\delta = -0.64$).

Example 2. (*Comparison with recent techniques in presence of unstructured-bounded noise*) In this example, the proposed method equipped by a prefilter $G_f(s) = \frac{s}{s+100}\frac{300}{s+300}$ is compared with two recent AFP techniques proposed in [17] and [24] respectively. All the methods are discretized by the Euler method with identical sampling period 10μs.

Consider a measured signal $y(t)$ affected by an unstructured disturbance, which is a norm-bounded time-varying signal:

$$\hat{y}(t) = y_0(t) + A^*(t)\sin\Big(\int 2\pi f^*(\tau)d\tau + \phi^*(t)\Big) + \eta(t), \quad (34)$$

with $\eta(t)$ denotes the bounded uncertainty with uniform distribution in the interval $[-0.25, 0.25]$. The other parameters start from $f^*(0) = 60$Hz, $A^*(0) = 1$, $y_0(0) = \phi^*(0) = 0$, and jump to $f^*(t) = 60.4$Hz, $A^*(t) = 1.2$, $y_0(t) = -0.1$, $\phi^*(t) = \frac{\pi}{2}$ at time $t = 0.3s$. At time $t = 1.4$s, a further step-wise variation of the parameters occurs: $f^*(t) = 59.5$Hz, $A^*(t) = 0.9$, $y_0(t) = 0.2$, $\phi^*(t) = -\frac{\pi}{4}$.

All the methods are initialized with the same initial

condition $\hat{\omega}(0) = 1$. Method [17] is tuned with: $K_s = 1$, $\lambda = 30$, $\omega_s = 60$, $Q_0 = (1/\lambda)\mathbf{I}$, while method [24] is tuned with: $\lambda = 60$, $\beta = 0.6$, $\mu = 0.3$. The tuning parameters of the proposed GEPLL are fixed by: $\mu_A = \mu_\vartheta = 300$, $\mu_\omega = 15000$, $\delta = -0.64$.

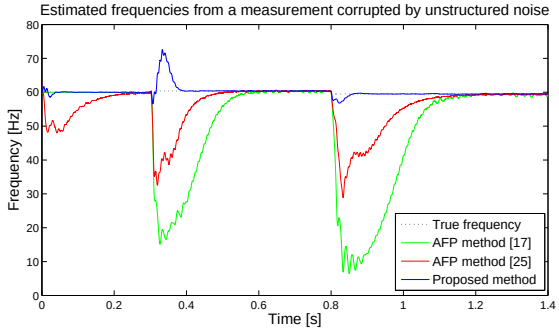

Fig. 3. Time-behavior of the estimated frequency by using the proposed GEPLL (blue line) compared with the time behaviors of the estimated frequency by the AFP methods [17] (green line) and [24] (red line).

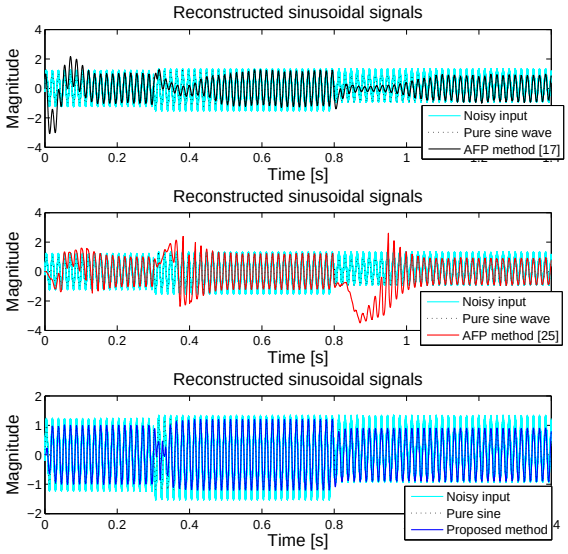

Fig. 4. Time-behavior of the reconstructed sine wave by using the proposed AFP methods (blue line) compared with the time behaviors of the estimated frequency by the AFP methods [17] (black line) and [24] (red line).

According to the results given in Fig.3, all the methods are capable to deal with the step-wise parametric changes, and to asymptotically recover the original sine wave in presence of high-frequency disturbances. However, the GEPLL shows a much faster transient behavior (with comparable steady state performance) than the other two approaches. As a consequence, Fig. 4 enhances the significantly improved synchronization with respect to the pure sinusoid yielded by the proposed GEPLL, whereas methods [17] and [24] slightly suffer from the parametric variations.

V. Concluding Remarks

In the paper, an enhanced phase-locked loop algorithm with generalized error filtering has been presented. This technique allows to estimate the parameters of a sinusoidal signal in presence of biased measurements and high-frequency perturbations, while maintaining the immediacy of implementation that characterizes the PLL architecture and maintaining transient response swiftness, as well. A stability analysis has been carried out to determine the effect of the tuning parameters on the convergence behavior of the proposed algorithm. The steady-state and transient improvements over existing EPLL and bias-cancelling EPLL schemes are shown by comparative numerical examples.

References

[1] M. Karimi-Ghartemani and M. Iravani, "A nonlinear adaptive filter for online signal analysis in power systems: Applications," *IEEE Trans. on Power Delivery*, vol. 17, no. 2, pp. 617–622, 2002.

[2] M. D. Kusljevic, "A simple recursive algorithm for simultaneous magnitude and frequency estimation," *IEEE Trans. on Instrumentation and Measurement*, vol. 57, no. 6, pp. 1207–1214, 2008.

[3] S. Xue and S. Yang, "Power system frequency estimation using supervised gauss newton algorithm," *Measurement*, vol. 42, pp. 28–37, 2008.

[4] M. Mojiri, D. Yazdani, and A. Bakhshai, "Robust adaptive frequency estimation of three-phase power systems," *IEEE Trans. Instrum. Meas*, vol. 59, no. 7, pp. 1793–1802, 2010.

[5] M. Bodson, J. S. Jensen, and S. C. Douglas, "Active noise control for periodic disturbances," *IEEE Trans. on control systems technology*, vol. 9, no. 1, pp. 200–205, 2001.

[6] G. Pin, T. Parisini, and M. Bodson, "Robust parametric identification of sinusoidal signals: an input-to-state stability approach," in *Proc. IEEE Conference on Decision and Control and European Control Conference (CDC-ECC)*, 2011, pp. 6104–6109.

[7] X. Xia, "Global frequency estimation using adaptive identifiers," *IEEE Trans. on Automatic Control*, vol. 47, no. 7, pp. 1188–1193, 2002.

[8] M. Hou, "Estimation of sinusoidal frequencies and amplitudes using adaptive identifier and observer," *IEEE Trans. on Automatic Control*, vol. 52, no. 3, pp. 493–499, 2007.

[9] M. Mojiri, M. Karimi-Ghartemani, and A. Bakhshai, "Estimation of power system frequency using an adaptive notch filter," *IEEE Trans. Instrum. Meas*, vol. 56, no. 6, pp. 2470–2477, 2007.

[10] H.Hajimolahoseini, M. Taban, and H. Soltanian-Zadeh, "Extended kalman filter frequency tracker for nonstationary harmonic signals," *Measurement*, vol. 45, no. 1, pp. 126–132, 2012.

[11] F. Gardner, *Phaselock Techniques*. New York/Oxford: Wiley-Blackwell, 2005.

[12] G. Pin, "A direct approach for the frequency-adaptive feedforward cancellation of harmonic disturbances," *IEEE Trans. Signal Processing*, vol. 58, no. 7, pp. 3513–3530, 2010.

[13] L. Feola, R. Langella, and A. Testa, "On the effects of unbalances, harmonics and interarmonics in PLL systems," *IEEE Trans. on Instrumentation and Measurement*, vol. 62, no. 9, pp. 2399–2409, 2013.

[14] S. V. Aranovskii, A. A. Bobtsov, A. S. Kremlev, and G. V. Lukyanova, "A robust algorithm for identification of the frequency of a sinusoidal signal," *Journal of Computer and Systems Sciences International*, vol. 46, no. 3, pp. 371–376, 2007.

[15] S. Aranovskiy, A. Bobtsov, A. Kremlev, N. Nikolaev, and O.Slita, "Identification of frequency of biased harmonic signal," *European J. Control*, vol. 2, pp. 129–139, 2010.

[16] A. Bobtsov, D. Efimov, A. Pyrkin, and A. Zolghadri, "Switched algorithm for frequency estimation with noise rejection," *IEEE Trans. on Automatic Control*, vol. 57, no. 9, pp. 2400–2404, 2012.

[17] G. Fedele and A. Ferrise, "Non adaptive second order generalized integrator for identification of a biased sinusoidal signal," *IEEE Trans. Automatic Control*, vol. 57, no. 7, pp. 1838–1842, 2012.

[18] M. Hou, "Parameter identification of sinusoids," *IEEE Trans. on Automatic Control*, vol. 57, no. 2, pp. 467–472, 2012.

[19] B. Wu and M. Bodson, "A magnitude/phase-locked loop approach to parameter estimation of periodic signals," *IEEE Transactions on Automatic Control*, vol. 48, pp. 612–618, 2003.

[20] M. Karimi-Ghartemani and A. Ziarani, "Periodic orbit analysis of two dynamical systems for electrical engineering applications," *Journal of Engineering Mathematics*, vol. 45, no. 2, pp. 135–154, 2003.

[21] M. Karimi-Ghartemani, S. Khajehoddin, P. Jain, A. Bakhshai, and M. Mojiri, "Addressing dc component in PLL and notch filter algorithms," *IEEE Trans. on Power Electronics*, vol. 27, no. 1, pp. 78–86, 2012.

[22] M. Karimi-Ghartemani and M. Iravani, "Measurement of harmonics/inter-harmonics of time-varying frequencies," *IEEE Trans. on Power Delivery*, vol. 20, no. 1, pp. 23–31, 2005.

[23] S. Sastry and M. Bodson, *Adaptive Control: Stability, Convergence, and Robustness*. Prentice-Hall, 1994.

[24] G. Pin, B. Chen, T. Parisini, and M. Bodson, "Robust sinusoid identification with structured and unstructured measurement uncertainties," *IEEE Trans. on Automatic Control*, vol. 59, no. 6, pp. 1588–1593, 2014.